

# The MEP-1 zinc-finger protein acts with MOG DEAH box proteins to control gene expression via the *fem-3* 3' untranslated region in *Caenorhabditis elegans*

MARCO BELFIORE,<sup>1</sup> LAURA D. MATHIES,<sup>2,3</sup> PAOLO PUGNALE,<sup>1</sup> GARY MOULDER,<sup>4</sup>  
ROBERT BARSTEAD,<sup>4</sup> JUDITH KIMBLE,<sup>2,3</sup> and ALESSANDRO PUOTI<sup>1</sup>

<sup>1</sup>Department of Zoology, University of Fribourg, Pérolles, CH-1700 Switzerland

<sup>2</sup>Department of Biochemistry, University of Wisconsin–Madison, Madison, Wisconsin 53706, USA

<sup>3</sup>Howard Hughes Medical Institute, University of Wisconsin–Madison, Madison, Wisconsin 53706, USA

<sup>4</sup>Program in Molecular Biology, Oklahoma Medical Research Foundation, Oklahoma City, Oklahoma 73104, USA

## ABSTRACT

Cell fates in the *Caenorhabditis elegans* germline are regulated, at least in part, at the posttranscriptional level. For example, the switch from spermatogenesis to oogenesis in the hermaphrodite relies on posttranscriptional repression of the *fem-3* mRNA via its 3' untranslated region (UTR). Previous studies identified three DEAH box proteins, MOG-1, MOG-4, and MOG-5, that are critical for the *fem-3* 3' UTR control. Here we describe MEP-1, a zinc-finger protein that binds specifically to each of these three MOG proteins and that is required for repression by the *fem-3* 3' UTR in vivo. To investigate its in vivo function, we generated a *mep-1* deletion mutant. The *mep-1* null phenotype suggests a broad role for MEP-1 in *C. elegans* development, as it is associated with early larval arrest. In addition, *mep-1* mutants can be defective in gonadogenesis and oocyte production when derived from a heterozygous mother. We suggest that MEP-1 acts together with the MOG proteins to repress *fem-3* mRNA and that it also functions in other pathways to control development more broadly.

**Keywords:** posttranscriptional regulation; protein–protein interaction; protein–RNA interaction; sex determination; *trans*-acting factor

## INTRODUCTION

Posttranscriptional controls of gene expression are critical for metazoan development, particularly in the germline and the early embryo (Wickens et al., 2000). Such controls are most commonly mediated by regulatory *cis*-acting elements located in the 5' or 3' untranslated region (UTR) of the regulated mRNA. The mechanisms by which these regulatory sites control mRNA activity are however, for the most part, not well understood. In the nematode *Caenorhabditis elegans*, 3'-UTR-mediated regulation influences identity of embryonic blastomeres (Evans et al., 1994; Mickey et al., 1996), progression through larval development (Lee et al., 1993; Moss et al., 1997; Slack et al., 2000) and sex determination in the germline (Ahringer & Kimble, 1991;

Goodwin et al., 1993). Our focus has been on the germline, with a specific emphasis on the control of *fem-3* mRNA and the sperm/oocyte switch.

*C. elegans* can exist either as a male, which produces sperm continuously, or as a hermaphrodite, which transiently makes sperm during larval development and switches to oogenesis as an adult. The switch from spermatogenesis to oogenesis depends on the posttranscriptional control of *fem-3*, a sex-determining gene that promotes male development (Hodgkin, 1986; Barton et al., 1987). Within the *fem-3* 3' UTR resides a regulatory element, called PME, that is crucial for the sperm/oocyte switch (Ahringer & Kimble, 1991). Lesions in the PME abolish repression of the *fem-3* RNA, causing a failure in the switch from spermatogenesis to oogenesis, an accumulation of excess sperm and an absence of oocytes in the adult hermaphrodite (Barton et al., 1987; Ahringer & Kimble, 1991).

In a previous study, we identified six *mog* genes (Graham & Kimble, 1993; Graham et al., 1993). Be-

Reprint requests to: Alessandro Puoti, Department of Zoology, University of Fribourg, Pérolles, CH-1700 Switzerland; e-mail: Alessandro.Puoti@unifr.ch.

cause animals lacking the activity of any one of the *mog* genes fail to switch from spermatogenesis to oogenesis, each *mog* gene is essential for the sperm/oocyte switch. In addition, all six *mog* genes are critical for regulation by the *fem-3* 3' UTR (Gallegos et al., 1998). Three *mog* genes have been cloned: *mog-1*, *mog-4*, and *mog-5* (Puoti & Kimble, 1999, 2000). Intriguingly, all three MOG proteins are homologous to yeast pre-mRNA splicing factors: MOG-1 is homologous to Prp16p, MOG-4 to Prp2p, and MOG-5 to Prp22p. For the purposes of this work, we refer to MOG-1, MOG-4, and MOG-5 as "the MOG proteins."

In addition to the *mog* genes, we sought RNA-binding proteins that bind specifically to the *fem-3* PME (Zhang et al., 1997). In this way, we identified FBF-1 and FBF-2, two nearly identical proteins. Both FBF-1 and FBF-2 bind the wild-type PME, and that binding is abolished in mRNAs that contain mutations in the PME. Furthermore, a reduction of both *fbf-1* and *fbf-2* by RNA-mediated interference leads to a failure in the sperm/oocyte switch (Zhang et al., 1997). The two *C. elegans* FBF proteins belong to the Puf family, which includes *Drosophila* Pumilio. Screens for FBF-interacting proteins identified NOS-3, which appears to act together with FBF in the sperm/oocyte switch (Kraemer et al., 1999). Our working model has been that binding of FBF and NOS-3 to the *fem-3* 3' UTR leads to the repression of *fem-3* mRNA activity. The mechanism is likely to involve a decrease in polyadenylation and repression of translation (Ahringer & Kimble, 1991).

FBF and NOS-3 are predominantly cytoplasmic (Zhang et al., 1997; Kraemer et al., 1999), but the three MOG proteins are nuclear and do not bind the PME repressor element (Puoti & Kimble, 1999, 2000; A. Puoti, unpubl. observations). The molecular mechanism by which the MOG proteins control *fem-3* mRNA activity is therefore much less clear than that proposed for FBF and NOS-3. In an attempt to learn how the *mog* genes control *fem-3* via its 3' UTR, we sought proteins that interact with the MOG proteins and that are also critical for *fem-3* regulation. Here we report the identification of MEP-1, a predicted zinc-finger protein that binds each of the three MOG proteins. Like the MOG proteins, MEP-1 is localized to the nucleus and is expressed in both somatic and germline tissues. Using a reporter transgene linked to the *fem-3* 3' UTR, we have shown that *mep-1* is required for *fem-3* 3' UTR-mediated repression in vivo. In vitro, we find that MEP-1 binds RNA nonspecifically. To explore *mep-1* function in vivo, we used a combination of RNA interference (RNAi) and characterization of a deletion mutant. In this way, we found that *mep-1* is required broadly during development for larval viability, gonadal morphogenesis, oocyte production, and germ cell proliferation. We also show that the FBF-1 protein is normally expressed in *mep-1* mutants, indicating that *mep-1* does not repress *fem-3* by promoting *fbf-1* expression. We propose that

the MOG proteins might assemble with MEP-1 to form a nuclear complex that is required for *fem-3* repression.

## RESULTS

### Identification of *mep-1*

To search for interacting partners of MOG-1 and MOG-5, full-length MOG proteins were fused to the DNA-binding domain of LexA and used as baits in yeast two-hybrid screens. We screened 400,000 and 450,000 independent cDNA clones of a *C. elegans* library with MOG-1 and MOG-5, respectively. In both screens, cDNAs encoding a protein with seven putative zinc fingers were obtained. This protein was termed MEP-1 (for MOG interacting and ectopic P-granules) because of its ability to bind the MOG proteins (this work), and because P-granules accumulate ectopically in *mep-1* deficient animals (Y. Unhavaithaya & C. Mello, submitted). The *mep-1* gene is located between *lin-3* and *let-60* on chromosome IV, and does not correspond to any of the six *mog* genes, which all map to chromosomes II and III (Graham et al., 1993). A comparison of the *mep-1* genomic sequence to that of the *mep-1* cDNA sequences provided an exon/intron map of the *mep-1* gene (Fig. 1A). Five independent *mep-1* cDNAs were obtained as MOG-1-interactors, and 14 as MOG-5-interactors (Fig. 1B). To verify that MEP-1 does not bind proteins nonselectively, we performed a two-hybrid screen using full-length MEP-1 as bait. Out of 120,000 cDNAs screened, only 2 caused strong reporter activation, suggesting that MEP-1 is selective in protein binding. Although neither MOG-1 nor MOG-5 was found in the MEP-1 screen, one cDNA encoded full-length MEP-1, indicating that MEP-1 can interact with itself (Fig. 1B).

MEP-1 possesses seven predicted zinc fingers: one cluster of three zinc fingers is separated from a second cluster of four zinc fingers by a glutamine-rich region (Fig. 1B, residues 545–686 in Fig. 1C). Six zinc fingers have the canonical CCHH structure, and the third finger, counting from the N-terminus, is of the CCHC type (Fig. 1C). In addition, MEP-1 carries two potential nuclear localization signals (Fig. 1C). Database searches identified a *Drosophila* homolog (gene product CG1244, protein accession number AAF47669), which shares only 20% overall amino acid identity with *C. elegans* MEP-1, but has conserved residues throughout its entire length, retains all cysteines and histidines of all seven putative zinc fingers, and carries a glutamine-rich domain between the third and the fourth zinc fingers; no function has yet been attributed to *Drosophila* MEP-1. A similar homolog has not been identified in yeast or vertebrates.

Whereas screens with MOG-1 or MEP-1 yielded full-length or almost full-length *mep-1* cDNAs (Fig. 1B: MOG-1 screen, arrows; MEP-1 screen, arrows), screens

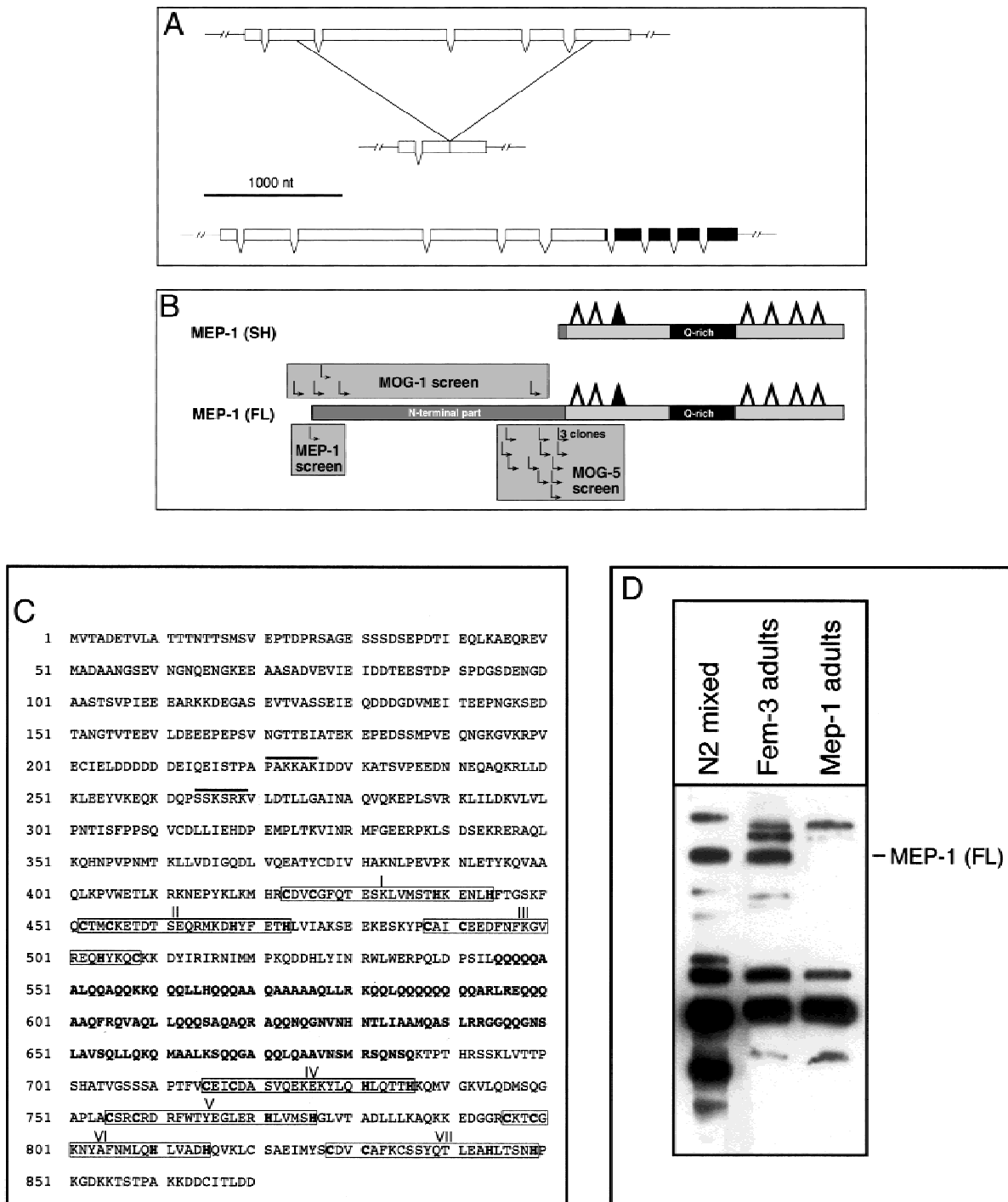


**FIGURE 1.** The *mep-1* gene and protein products. **A:** The *mep-1* gene and variants: Top: the *mep-1* gene is shown with exons represented as boxes and introns as joining lines. Center: the *mep-1(q660)* deletion mutant removes 2,183 nt and fuses the 5' portion of exon 2 with the 3' portion of exon 6. This deletion removes the region encoding the seven zinc fingers and the Q-rich domain. Bottom: the *mep-1::GFP* construct. The GFP gene was fused in frame to the 3' end of the last exon in *mep-1*. GFP exons are shaded; 5' and 3' flanking regions are 2,363 and 778 nt, respectively, and are not drawn to scale. Bar: 1,000 nt. **B:** Two predicted MEP-1 proteins. Top: MEP-1(SH) and MEP-1(FL) both carry seven zinc fingers (triangles) and a Q-rich domain (dark gray). The CCHC zinc finger is represented by a filled triangle. Shaded boxes indicate the clones that were obtained by different two-hybrid screens (MOG-1, MOG-5, and MEP-1); arrows within the shaded boxes indicate the 5' ends of independently isolated cDNAs. **C:** Amino acid sequence of MEP-1. The Q-rich domain is shown in bold and the zinc fingers are boxed and numbered I to VII; cysteines and histidines in the backbone of the zinc fingers are shown in bold letters. Two predicted nuclear localization signals in the N-terminus are overlined. Sequence data for the *mep-1* cDNA are accessible under number AAL27004. **D:** Total protein extracts from wild-type worms at mixed developmental stages (wild-type mixed), feminized (Fem-3), and Mep-1 adults were separated by SDS-PAGE, blotted, and probed with affinity-purified polyclonal MEP-1 antibodies. MEP-1 corresponds to one single product running at 115 kDa that is present in both wild-type and Fem-3 animals but that is absent in *mep-1* mutants.

with MOG-5 yielded shorter cDNAs (Fig. 1B: MOG-5 screen, arrows). This difference might be explained by the existence of a shorter protein, MEP-1(SH) (Fig. 1B) and by a block of MOG-5 binding to full-length MEP-1 protein (see below). The shortest cDNA obtained in the MOG-5 screen is predicted to generate a protein that nonetheless retains all zinc fingers and the glutamine-rich domain. Affinity-purified MEP-1 antibodies identified several products in crude protein extracts from wild-type worms at different developmental stages and feminized Fem-3 adults (Fig. 1D). However, only one protein of 115 kDa was absent in *mep-1(q660)* mutant adults and is therefore likely to correspond to full-length MEP-1 (Fig. 1D, lane 3). We did not identify shorter isoforms of MEP-1 that were present in both wild-type and feminized animals and were absent in the *mep-1* mutant, indicating that MEP-1(SH) is not present in wild-type worms, at least at a level that can be detected by western analysis.

### MEP-1 physically interacts with three MOG proteins and itself

We next examined systematically the interactions among MOG proteins and MEP-1 by two-hybrid assays. In these studies, we included MOG-4, a third DEAH box protein identified in a parallel study (Puoti & Kimble, 2000), but not used in two-hybrid screens. We found that MEP-1(FL) interacted with MOG-1, MOG-4, and with itself, but not with MOG-5 (Fig. 2A, top row, columns 1–4). Interactions between MEP-1(FL) and the MOG proteins are specific, because MEP-1(FL) did not interact with FBF-1, NOS-3, or GLD-1 (Fig. 2A, top row, column 5; data not shown for NOS-3 and GLD-1). By contrast, MEP-1(SH) interacted with all three MOG proteins, but not with MEP-1(FL) or FBF-1 (Fig. 2A, bottom row) and it did not interact with NOS-3 (data not shown). For MEP-1(FL), the interactions reported in Figure 2A were confirmed in the opposite orientation (e.g., with a MEP-1::LexA fusion; data not shown). For MEP-1(SH), the reverse experiment could not be done because MEP-1(SH) caused autoactivation of the reporter as a LexA fusion (data not shown).

To confirm the results from the yeast two-hybrid assays, we analyzed binding in vitro (Fig. 2B). To this end, MEP-1 fused to glutathione-S-transferase (GST) and carried on glutathione Sepharose™ beads was incubated with <sup>35</sup>[S]-labeled MOG or MEP proteins. Retained proteins were examined by gel electrophoresis. Beads with GST alone or GST-FBF were used as negative controls. We found that MOG-1 binds specifically in vitro with either short or full-length MEP-1-GST fusion proteins, but neither with GST alone, nor FBF-1-GST, indicating that the binding is specific (Fig. 2B, not shown). Similarly, MOG-4, MOG-5, and MEP-1(FL) bind both full-length and short MEP-1-GST fusion proteins (Fig. 2B). The in vitro binding confirms the two-hybrid

interactions with two exceptions: in vitro, MEP-1(FL) binds MOG-5 and MEP-1(SH), whereas this is not the case in the yeast two-hybrid assay. The observation that MEP-1(FL) and MOG-5 do not bind in yeast, but do so in vitro might result from a difference in MEP-1 conformation or the amounts of protein available when assayed by these distinct methods.

We next asked if the MOG proteins interact among themselves. For this study, we used fusions between the LexA DNA binding domain and cDNAs encoding each full-length MOG protein as well as fusions between the Gal4 activation domain and the following full-length cDNAs: *mog-1*, *mog-4*, *mog-5*, *fbf-1*, *fbf-2*, and *nos-3*. Only one interaction was observed in this matrix (Fig. 2C; data not shown for FBF-2). MOG-1 and MOG-4 coexpression activated the reporter transgene (Fig. 2C, column 1, row 2, and column 2, row 1), but this interaction was found to be RNA dependent (see below). The slight blue color detected in yeast expressing MOG-5::LexA is background (Fig. 2C, column 3, see also Fig. 2A, row 1, column 3), as it was also observed in strains transformed with *mog-5*::LexA alone (data not shown).

### MEP-1 is an RNA-binding protein, but does not require RNA for MOG interactions

Because the MOG proteins are required for control by the *fem-3* 3' UTR, but do not bind to the *fem-3* 3' UTR, we asked whether MEP-1 might bind the *fem-3* 3' UTR. To this end, we used a yeast three-hybrid assay with the following elements: (1) The DNA binding portion of LexA fused to the MS2 RNA-binding protein (SenGupta et al., 1996); (2) The MS2 RNA fused to the test RNA (Zhang et al., 1997); and (3) The Gal4 activation domain fused to either MEP-1(FL) or MEP-1(SH). As shown in Figure 3A, no interaction was observed if the hybrid RNA was omitted (row 1), suggesting that MEP-1 alone cannot bind MS2 coat protein via nonspecific protein–protein interactions. As a positive control, we used the IRP protein and an IRE as RNA partner, which physically interact (Fig. 3A; SenGupta et al., 1996). We then tested MEP-1(FL) and MEP-1(SH) for binding a variety of RNAs, including the wild-type *fem-3* 3' UTR, two mutant *fem-3* 3' UTRs (*q96* and *chg8*) that abrogate 3' UTR regulation, and an iron responsive element. In all cases, MEP-1(FL) or MEP-1(SH) interacted with the hybrid RNAs, suggesting that MEP-1 can bind to different RNAs (Fig. 3A, data not shown for short MEP-1).

Because MEP-1 binds RNA nonspecifically and because preparation of in vitro-translated proteins contain many RNAs, we considered the idea that interactions observed in vitro might depend on nonspecific protein–RNA binding, rather than being specific protein–protein interactions. To test this possibility, we treated the radiolabeled preparations with RNase before incu-

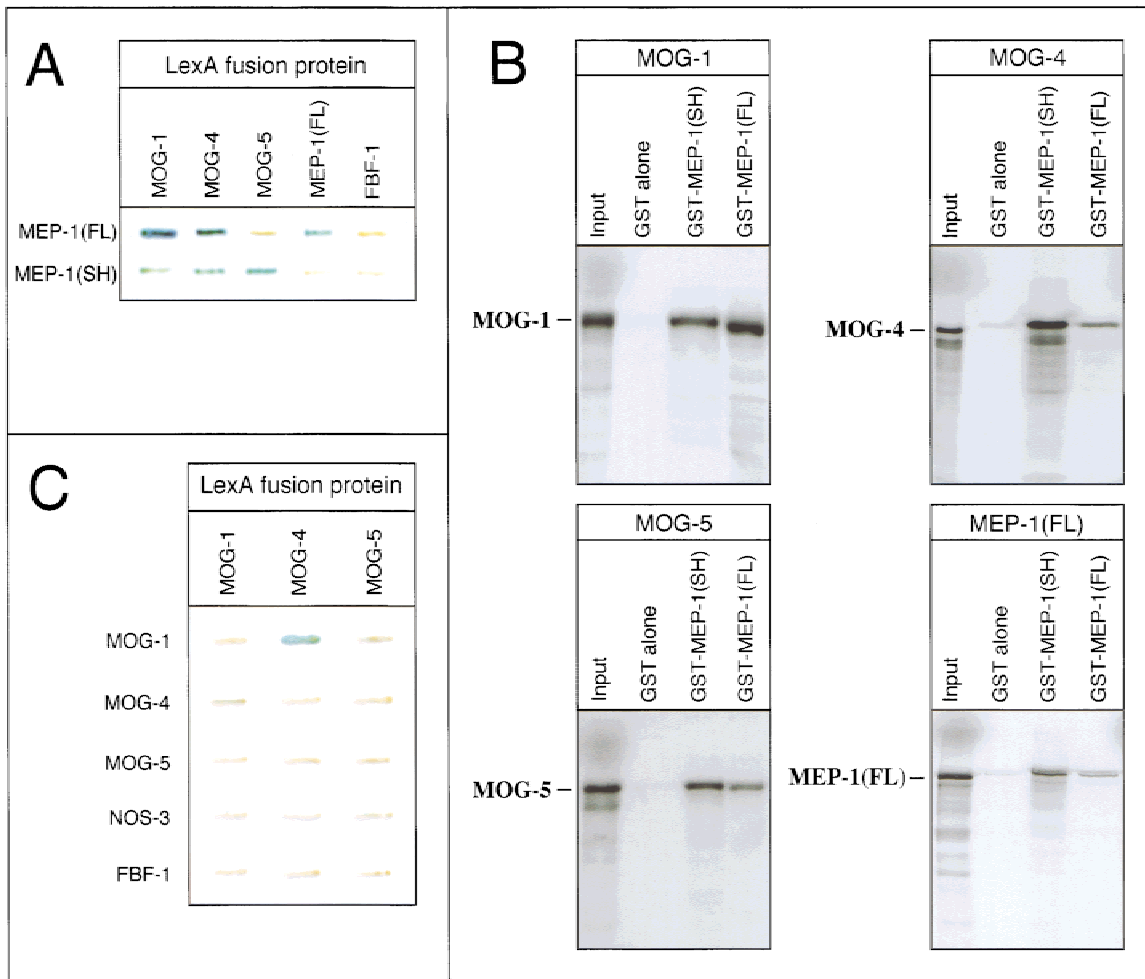


**FIGURE 2.** MEP-1 physically interacts with three MOG proteins and itself. **A:** Interactions between MEP-1 and the MOG proteins in a yeast two-hybrid assay. In the  $\beta$ -Gal filter assay, blue indicates a positive interaction between two proteins. MEP-1(FL) and MEP-1(SH) were fused the Gal4 activation domain. The slight blue color in column 3, top row, is due to autoactivation by MOG-5::Lex A fusion. MEP-1(FL) interacts with MOG-1, MOG-4, and MEP-1(FL) itself (top row). MEP-1(SH) interacts with the three MOG proteins (bottom row). FBF-1 is used as a negative control. **B:** MEP-1 and MOG interactions in vitro. Radiolabeled polypeptides that were retained on the GST beads were analyzed by SDS-PAGE. The input lane represents 10% of the amount of radiolabeled protein added to the binding reaction. The lane marked "GST alone" represents the amount of protein bound to beads loaded with GST that was not fused to MEP-1. **C:** Yeast two-hybrid assay for interactions among the MOG proteins. Each MOG protein was fused to LexA. In addition, the three MOG proteins, NOS-3, or FBF-1 were fused to the Gal4 activation domain. The signal observed in cells coexpressing MOG-1 and MOG-4 is due to protein-RNA interactions (see Fig. 3C). Otherwise, no interactions were observed in this matrix.

bation with Sepharose beads linked to MEP-1(SH)::GST or MEP-1(FL)::GST, and found that RNase treatment did not significantly reduce binding of MOG or MEP-1(FL) protein to the MEP-1::GST (Fig. 3B). Therefore, MOG-MEP and MEP-MEP interactions do not depend on nonspecific protein-RNA interactions.

We also tested whether the interaction between MOG-1 and MOG-4 was due to an RNA molecule that is unspecifically bound by two proteins. To this end, we treated in vitro-synthesized MOG proteins with RNase and found that RNase A treatment virtually abolished the binding of radiolabeled MOG proteins to GST-MOG-4 (Fig. 3C; compare lanes 1–3 with lanes 4–6). Therefore, the reporter activation in yeast expressing

MOG-1 and MOG-4 hybrids is likely to be due to protein-RNA rather than protein-protein interactions.

### *mep-1* mRNA and protein expression

By northern analysis, a single *mep-1* mRNA of 3.2 kb is expressed throughout development (Fig. 4A, lanes 1–6). The temporal profile of *mep-1* mRNA expression was similar to that observed for *mog-1*, *mog-4*, and *mog-5* mRNAs (Puoti & Kimble, 1999, 2000). Thus, the steady-state level of *mep-1* mRNA was highest in embryos, decreased during early larval development (L1–L3), and increased at the fourth larval stage (L4). The *mep-1* mRNA was present in wild-type adults, but its level was

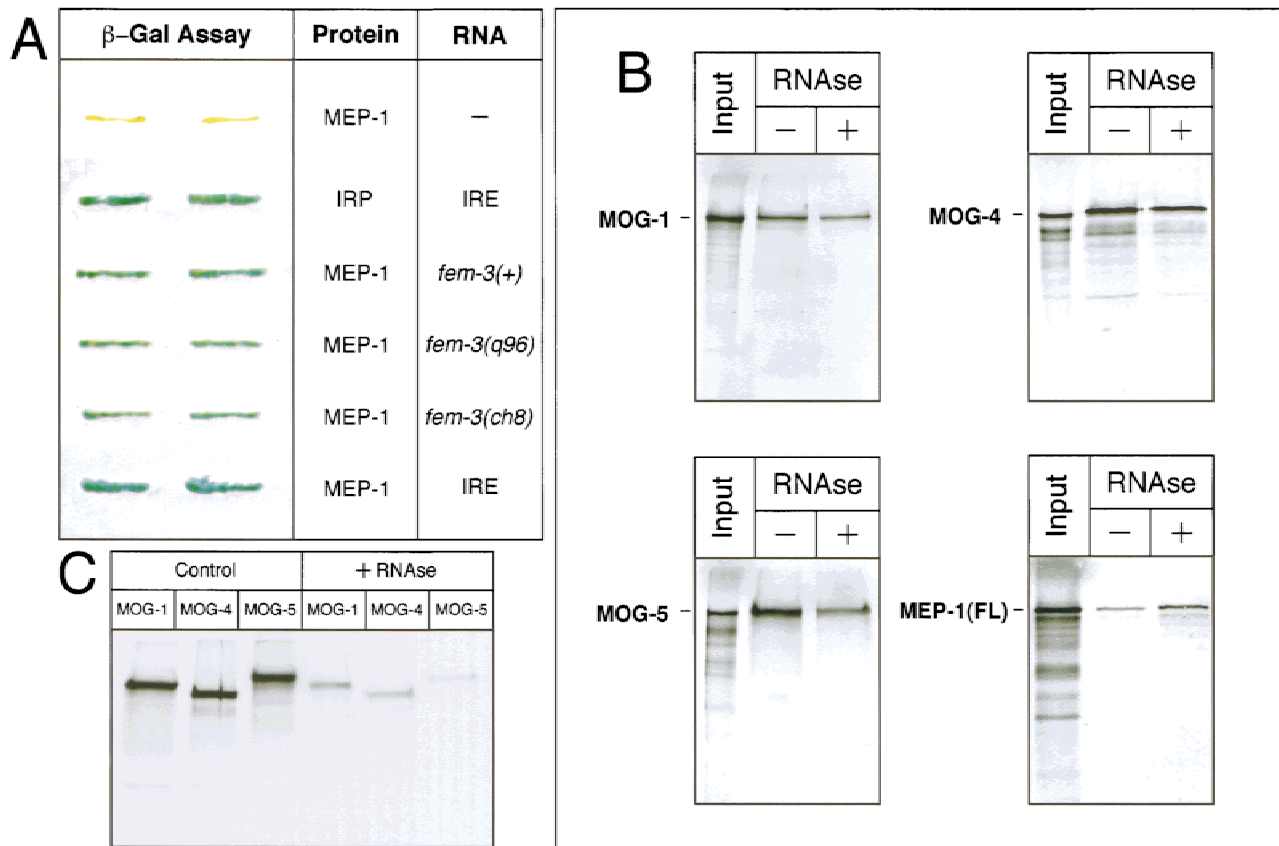


**FIGURE 3.** MEP-1 is a nonspecific RNA-binding protein. **A:** MEP-1 binds RNA nonspecifically when assayed by the yeast three-hybrid system. The  $\beta$ -Gal filter assay shows the interaction between MEP-1 and different RNAs. No RNA was present in row 1. As a positive control for protein–RNA interaction, we used the iron-responsive binding protein (IRP) and an iron responsive element (IRE, row 2). Positive interaction is indicated by blue color. Rows 3 to 5 show that MEP-1 is able to bind to the wild-type *fem-3* 3' UTR, but also to *fem-3* RNAs with one (*fem-3(q96)*) or eight (*fem-3(ch8)*) point mutations that modify the sequence of the wild-type PME. Row 6 shows the positive interaction between MEP-1 and the IRE RNA. This panel represents the results obtained using two independent transformants. **B:** Effect of RNase on in vitro protein–protein interactions: In vitro translated and [<sup>35</sup>S]-labeled proteins were either mock incubated (–) or treated with RNase (+) before being added to beads loaded with GST-MEP-1(FL). Short MEP-1 was used for the interactions between MOG and MEP-1 and full-length MEP-1 was used for the interaction with MEP-1. No significant effect of the RNase treatment has been observed. The input corresponds to 10% of radiolabeled protein that was added to the binding reaction. **C:** MOG proteins bind RNA in vitro. In vitro-synthesized and radiolabeled MOG-1, -4, or -5 proteins were either mock incubated (control) or treated with RNase (+RNase) before being added to beads loaded with MOG-4-GST. The signals correspond to the proteins that were retained on the beads. RNase treatment greatly reduced the binding of MOG-1, MOG-4, and MOG-5, suggesting that MOG proteins interact with each other via an RNA bridge.

dramatically reduced in *gfp-1(q224)* adults, which lack a germline (Austin & Kimble, 1987; Fig. 4A, compare lanes 6 and 7). The *mep-1* transcript is therefore abundant in the hermaphrodite germline, but is also present in somatic tissues, as also observed for the three *mog* transcripts (Puoti & Kimble, 1999, 2000).

The apparent somatic expression of *mep-1* mRNA and the predicted nuclear localization signals in the MEP-1 sequence led us to investigate expression of a MEP-1::GFP fusion protein in somatic tissues. To this end, we generated transgenic animals carrying *mep-1::GFP*, a transgene with the *GFP* gene fused in frame to the 3' end of the last *mep-1* exon (Fig. 1A, bottom). This construct rescues a *mep-1(q660)* mutant, suggesting that its expression mimics that of endogenous *mep-1*. In wild-type animals, *mep-1::GFP* was expressed in

most somatic cells in embryos (Fig. 4B) and young larvae (Fig. 4C); however, the GFP reporter construct did not express in a subset of embryonic cells that give rise to the central part of the worm (Fig. 4B). Later during larval development, expression was consistently detected in cells of the head, the hypodermis, and the tail (Fig. 4D, E, tail not shown). In all cases, MEP-1::GFP was nuclear. Because the expression of transgenes is silenced in the germline, we did not interpret the absence of *mep-1::GFP* from the germline as indicative of its expression. To study *mep-1* expression in the germline, we generated polyclonal antibodies to the C-terminal portion of MEP-1. By immunolocalization, MEP-1 was found in all nuclei in the germline, including oocytes, but not those of mature sperm and spermatocytes (Fig. 4F, G). The ab-

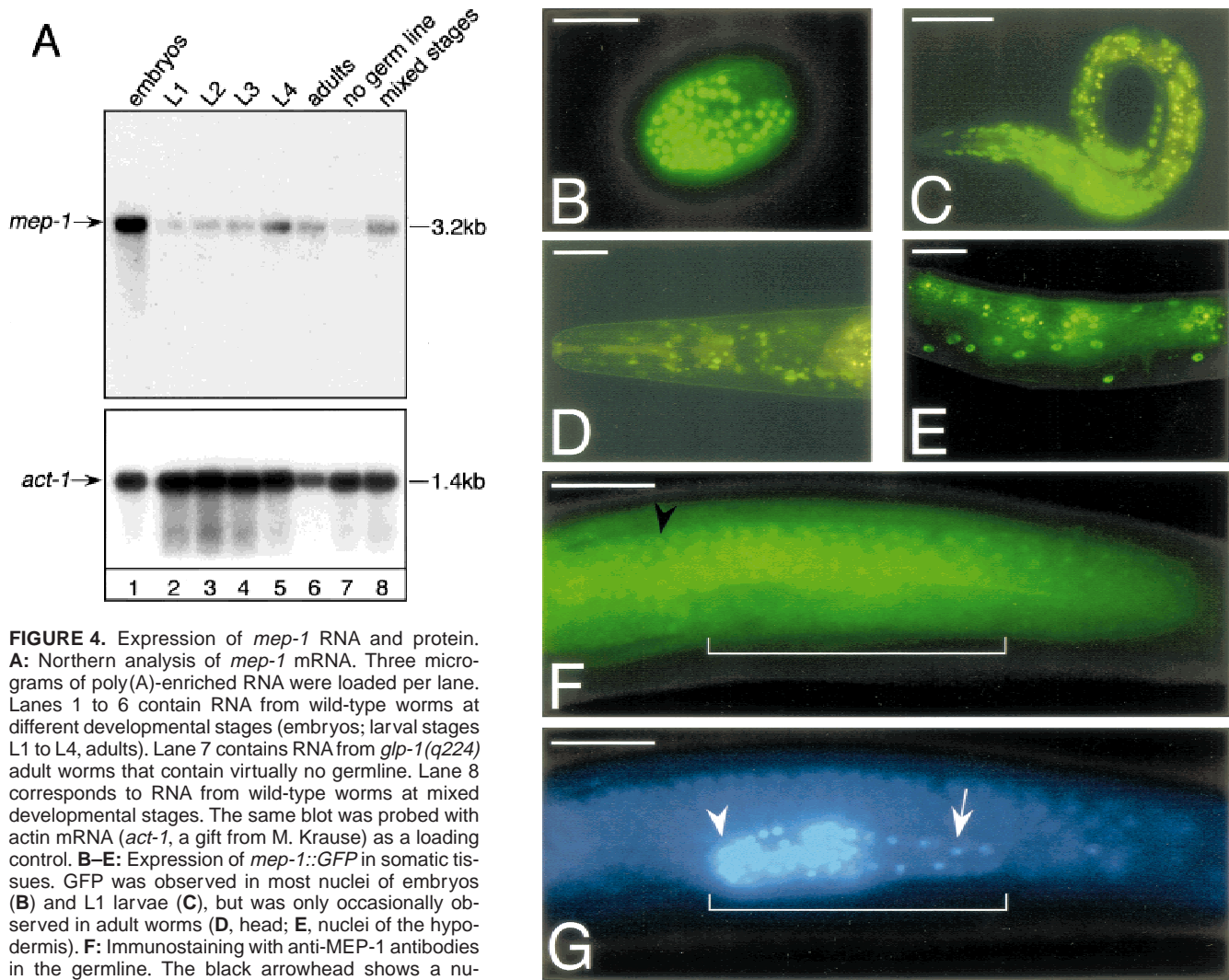


**FIGURE 4.** Expression of *mep-1* RNA and protein. **A:** Northern analysis of *mep-1* mRNA. Three micrograms of poly(A)-enriched RNA were loaded per lane. Lanes 1 to 6 contain RNA from wild-type worms at different developmental stages (embryos; larval stages L1 to L4, adults). Lane 7 contains RNA from *glp-1(q224)* adult worms that contain virtually no germline. Lane 8 corresponds to RNA from wild-type worms at mixed developmental stages. The same blot was probed with actin mRNA (*act-1*, a gift from M. Krause) as a loading control. **B–E:** Expression of *mep-1::GFP* in somatic tissues. GFP was observed in most nuclei of embryos (**B**) and L1 larvae (**C**), but was only occasionally observed in adult worms (**D**, head; **E**, nuclei of the hypodermis). **F:** Immunostaining with anti-MEP-1 antibodies in the germline. The black arrowhead shows a nucleus in the distal arm of the gonad. No staining is observed in the proximal region of the germline (white bracket). **G:** Nuclear DAPI staining of the animal in **F**. The bracket shows the region containing mature sperm (white arrowhead) and sperm precursors (white arrow) that have condensed nuclei. **F** and **G** are in the same focal plane and represent one gonadal arm of an L4 larva that has not started oogenesis. The bar represents 20  $\mu$ m. Anterior is to the left in **C** to **G**.

sense of MEP-1 in sperm and sperm precursors is in accordance with its role in repressing *fem-3*. Furthermore, no staining has been detected in male germlines (data not shown). This and the presence of MEP-1 in oocytes suggest that *mep-1* is required for female cell fates, but not male gametes. No staining has been detected in *mep-1(q660)* mutants, indicating that the antibody specifically recognizes MEP-1 and that *q660* represents a null allele (data not shown).

#### *mep-1* is an essential gene

We tested the biological function of *mep-1* both by RNA interference (Fire et al., 1991, 1998) and by generating

a *mep-1* deletion mutant. The *mep-1(q660)* deletion removes 2,183 nt of genomic sequence, including 1,965 coding nt (nt 357 to 2322 in the *mep-1* cDNA). The deletion ends before the normal *mep-1* stop codon and resumes in a different reading frame to create a premature stop codon 44 nt downstream of the deletion junction. Therefore, *mep-1(q660)* is predicted to encode 111 amino acids N-terminal to the deletion endpoint and an additional 14 amino acids C-terminally, which are different from those in the wild-type MEP-1 protein. Of most importance, the deletion removes 635 amino acids from the center of MEP-1, including all seven zinc fingers and the Q-rich region (Fig. 1A, middle drawing).

The *mep-1(q660)* mutant is temperature sensitive: defects are less severe at 15 °C than at 20 °C and 25 °C. At 15 °C, 72% of *mep-1* homozygotes derived from a heterozygous mother were sterile, and the remaining 28% were self-fertile ( $n = 64$ ); at 20 °C, 88% were sterile and 12% arrested as young larvae ( $n = 115$ ); and at 25 °C, 99% arrested as young larvae (L1 or L2,  $n = 124$ ). At 15 °C, all *mep-1* homozygotes that had been derived from one of the fertile *mep-1* homozygous mothers died as young larvae. Therefore, a wild-type copy of maternal *mep-1* can rescue *mep-1* larval lethality at 15 °C. Arrested larvae were also obtained by RNAi, a technique that interferes with both maternal and zygotic RNAs. Typically, among progeny from 10 wild-type hermaphrodites injected with double-stranded *mep-1* RNA, 83% arrested at an early larval stage, 15% were sterile adults, and 2% were fertile ( $n = 773$ ). Sterile *mep-1(RNAi)* progeny had the same phenotype as *mep-1* mutants grown at 20 or 25 °C.

### *mep-1* is required for somatic gonadal development

Somatic gonadal development is normal in *mog* mutants (Graham & Kimble, 1993; Graham et al., 1993). In contrast, somatic gonadal development is aberrant in sterile *mep-1* mutants and in *mep-1(RNAi)* animals. At 20 °C, the most common defect was a failure in gonadal arm elongation. In wild-type animals, the gonad forms an elongated U-shaped tube (Fig. 5A), but in *mep-1* mutants, elongation was arrested (Fig. 5B). At 25 °C, the most common defect was a failure in gonadal growth. Whereas wild-type gonads begin to grow in L1 and become an organ that fills the body cavity by adulthood (Kimble & Ward, 1988; Fig. 5C), *mep-1* mutant gonads contained only a few gonadal cells by L3 (Fig. 5D) or a small patch of gonadal tissue in adults (not shown). *mep-1* males had similar gonadal defects (data not shown).

To examine somatic gonadal defects in more detail, we counted the number of distal tip cells (DTCs) produced at 15 °C versus 25 °C in *mep-1* mutants. In wild type, the DTCs control gonadal elongation. At 15 °C, 88% of *mep-1(q660)* homozygotes had two DTCs ( $n = 26$ ), whereas at 25 °C, none had DTCs ( $n = 18$ ). We also counted somatic gonadal blast cells produced during early larval development. In wild type, the two somatic gonadal precursors (Z1 and Z4) generate 12 cells by L2/L3 lethargus (Kimble & Hirsh, 1979). In contrast, in *mep-1* mutants raised at 25 °C, Z1 and Z4 generated between two and five total descendants by a similar time of development (average = 2.8 cells,  $n = 19$ ). At 15 °C, *mep-1* mutants had nearly the wild-type number of somatic cells at L2/L3 lethargus (average = 11.8 cells,  $n = 5$ ). Therefore, the somatic gonadal defects are considerably more severe at 25 °C than at 15 °C. In addition to somatic gonadal defects, most *mep-1* mu-

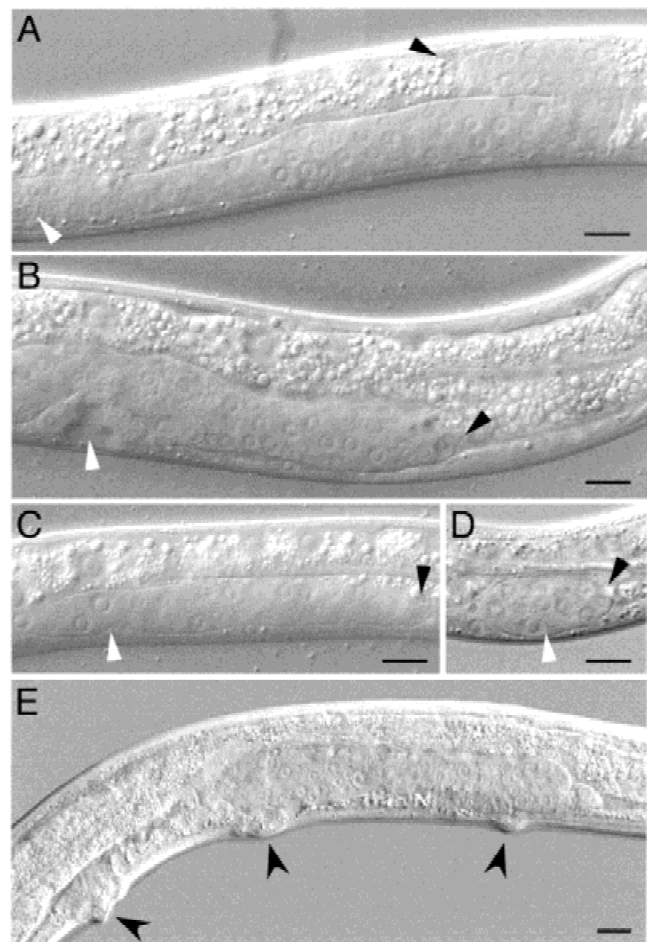


**FIGURE 5.** The Mep-1 mutant phenotype. In **A** to **D**, black arrowheads mark the distal tip of the gonad arm and white arrowheads mark the center of the gonad. **A:** Wild-type L4 hermaphrodite (20 °C); the gonadal arm has extended and reflexed normally. **B:** *mep-1* L4 hermaphrodite (20 °C); arm elongation is stunted. **C:** Wild-type L3 hermaphrodite (25 °C); the somatic gonad contains two DTCs and 10 somatic gonadal blast cells that cluster centrally. Arm elongation is normal. **D:** *mep-1* L3 hermaphrodite (25 °C); only two to five somatic gonadal cells are present and no gonadal elongation has occurred. **E:** *mep-1* adult hermaphrodite (20 °C); elongation has arrested; no oocytes are present; the number of germline cells is reduced. Three pseudovulvae are observed (arrowheads). The bar represents 10  $\mu$ m.

tants grown at 20 °C had a protruding vulva (Pvi; 80%,  $n = 53$ ), and some had one or two small pseudovulvae (15%,  $n = 53$ ; Fig. 5E). The additional vulvae were derived from P8.p (95%) or P4.p (1.7%) in the case of animals with one pseudovulva. The remaining 3.3% corresponded to animals with two pseudovulvae that showed induction of both P8.p and P4.p ( $n = 60$  worms scored). The vulval defects, which may be associated with a defective somatic gonad, were also temperature sensitive: at 15 °C, fewer mutants had everted (36%,  $n = 31$ ) or additional small vulvae (7%,  $n = 31$ ).

### Germline defects in *mep-1* mutants

To examine the *mep-1* mutant germline, we scored all progeny derived from *mep-1/+* heterozygotes by



Nomarski microscopy. At 20 °C, all adult *mep-1* homozygotes made sperm, but only 24% produced a few (2–6) oocytes, which were smaller than normal and never fertilized ( $n = 53$  worms); at 15 °C, the effect was less severe: 35% of *mep-1* homozygotes contained no oocytes and 65% had two to nine oocytes ( $n = 31$ ). Of the oocytes made at 15 °C, 16% were fertilized to make embryos that were not laid and therefore hatched in their mothers. Those progeny, however, did not develop beyond the first larval stage (L1). In addition, *mep-1* mutant adults have small germlines. Whereas wild-type XX adult hermaphrodites contain about 2,400 germ cells (Kimble & White, 1981), *mep-1* XX adults contained only  $771 \pm 88$  ( $n = 16$ ) germ cells, including sperm, at 15 °C and  $664 \pm 133$  ( $n = 24$ ) germ cells at 20 °C.

The *mep-1* somatic gonadal defects complicated our analysis of germline defects. In wild-type animals, DTCs are essential for germline proliferation (Kimble & White, 1981), and gonadal elongation is essential for development of somatic gonadal structures (Blelloch et al., 1999). In addition, sheath/spermatheca precursor cells or their descendants affect both germline proliferation and specification of sperm or oocytes (McCarter et al., 1997). We took two approaches to examine the *mep-1* effect on germline development in a more normal somatic gonad. First, we shifted *mep-1* mutants from 15 °C to 25 °C at a stage when key events of somatic gonadal development had occurred. Specifically, early L3 *mep-1* mutants were shifted from 15 °C to 25 °C, and their gonadal development scored as young adults. Among worms with two DTCs and normal-looking somatic gonads, 82.5% made sperm only and 17.5% had sperm and oocytes ( $n = 40$  gonadal arms). In a similar experiment, we counted how many sperm were generated in *mep-1* mutants that had been shifted from 15 °C to 25 °C. Although many worms were not making oocytes, the number of sperm was normal compared to wild type ( $302 \pm 42$  per worm;  $n = 17$ ).

The second approach was to examine the germline in *mep-1* homozygotes harboring the *mep-1::gfp* rescuing transgene, which expresses GFP in somatic but not germline tissues. In *C. elegans*, transgenes generated by the method used to make *mep-1::gfp* are generally silenced in the germline. To our surprise, *mep-1::gfp* rescued the *mep-1(q660)* germline defect better than somatic defects: at 20 °C, these animals were fertile but had somatic gonad defects and small broods. Therefore we have not been able to use the *mep-1* mutant to investigate the role of *mep-1* in the sperm/oocyte switch.

### The *mep-1* gene is required for *fem-3* 3'-UTR-mediated repression in somatic tissues

A previous study examined the role of *mog* genes in repression by the *fem-3* 3' UTR (Gallegos et al., 1998).

That study relied on somatic expression of a *lacZ* reporter transgene that was controlled by the wild-type *fem-3* 3' UTR. In wild-type worms, the reporter was repressed in somatic tissues, but in mutants for any of the six *mog* genes, it was derepressed. Therefore, the *mog* genes are active in somatic tissues and are critical for PME-mediated mRNA control (Gallegos et al., 1998). Given the physical interaction between MEP-1 and three MOG proteins, we wondered whether *mep-1* was also required for repression by the *fem-3* 3' UTR in vivo. To test this hypothesis, we constructed a *mep-1* strain that carried the *lacZ::fem-3* 3' UTR transgene as an integrated array. The resulting strain had the following progeny: 25% were *mep-1* homozygotes (*mep-1/mep-1*; *lacZ::fem-3* 3' UTR), 25% were wild type (+/+; *lacZ::fem-3* 3' UTR), and 50% were wild-type-looking *mep-1* heterozygotes (*mep-1/+*; *lacZ::fem-3* 3' UTR) as *mep-1(q660)* is a recessive allele. Worms picked among the progeny of *mep-1(q660)/+*; *lacZ::fem-3* 3' UTR were scored for *lacZ* expression. We found that wild-type worms had a reduced level of *lacZ* expression when compared to *mep-1/mep-1* mutants (Fig. 6A, B). To quantify *lacZ* expression levels, we counted the number of nuclei with strong staining in adult wild-type homozygotes (+/+), wild-type-looking heterozygotes (*mep-1/+*), and *mep-1* homozygotes (*mep-1/mep-1*). In three independent experiments, *mep-1* homozygotes exhibited strong staining in about two times more nuclei than their wild-type siblings [(1)  $44.8 \pm 17.2$  blue nuclei ( $n = 14$  worms scored), (2)  $70.8 \pm 25.9$  ( $n = 9$ ), and (3)  $43.8 \pm 14.6$  ( $n = 9$ ) in Mep-1 worms and (1)  $24.4 \pm 10.9$  ( $n = 17$ ), (2)  $43.4 \pm 16.3$  ( $n = 7$ ), and (3)  $21.3 \pm 10.3$  ( $n = 9$ ) in wild type worms respectively].

To verify that the derepression that we have observed was specific to the *fem-3* 3' UTR, we constructed a *mep-1* strain carrying the same transgene except that the *fem-3* 3' UTR was replaced by the *tra-2(+)* 3' UTR. Similar to *fem-3*, *tra-2* is also post-transcriptionally repressed through distinct elements, named TGEs (*tra* and Gli elements) located in the 3' UTR (Goodwin et al., 1993). In two independent experiments, we found strong repression of the transgene in both wild-type and Mep-1 adults. We counted  $5.0 \pm 4.8$  ( $n = 11$  worms scored) nuclei expressing  $\beta$ -Gal in Mep-1 worms and  $5.1 \pm 4.5$  ( $n = 12$ ) in wild-type worms, respectively in the first experiment (Fig. 6C, D). In the second experiment, the overall expression level was a little higher, but was similar in both wild-type [ $8.3 \pm 5.2$  ( $n = 32$ )] and Mep-1 animals [ $7.2 \pm 5.1$  ( $n = 21$ )]. These results indicate that *mep-1* does not act on the TGEs and that it specifically represses a transgene that carries the *fem-3(+)* 3' UTR. Therefore, the derepression of the PME-controlled transgene in *mep-1* mutants suggests that wild-type MEP-1 acts together with the MOG proteins to specifically control PME-mediated repression in somatic tissues in vivo.

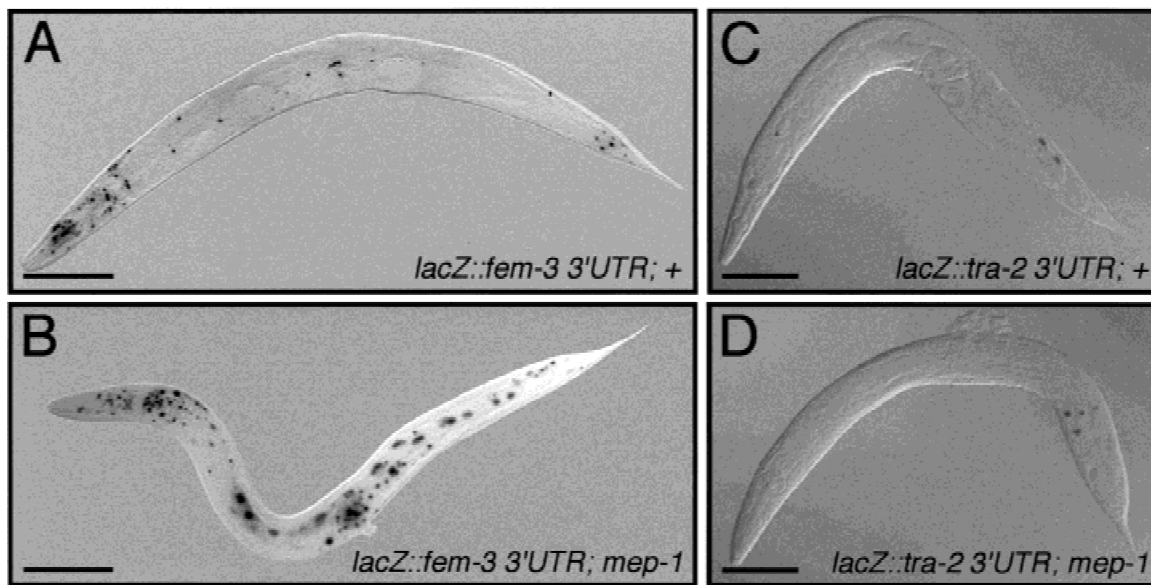


**FIGURE 6.** *mep-1* represses a *lacZ::fem-3 3' UTR* transgene in somatic tissues. The reporter *lacZ* is fused to the *fem-3 3' UTR* and includes a nuclear localization signal to ensure nuclear  $\beta$ -Gal. **A:** Fertile wild-type-looking animal of genotype  $+/+$ ; *lacZ::fem-3 3' UTR*, or *mep-1/+*; *lacZ::fem-3 3' UTR*. *lacZ* expression is present in the head and a few nuclei scattered throughout the body. **B:** *mep-1/mep-1::lacZ::fem-3 3' UTR*. *lacZ* expression is present in head and many nuclei scattered through the body. No increase of  $\beta$ -Gal expression was observed in *mep-1* animals carrying a similar transgene flanked by the *tra-2 3' UTR* (**C** and **D**). The large elongated structures in **B** represent intestinal nuclei expressing  $\beta$ -Gal. The bar represents 100  $\mu$ m. Anterior is to the left.

### Expression of FBF in *mep-1* hermaphrodites

In this study, we have shown that, similar to the *mog* genes and *fbf*, *mep-1* is required for *fem-3* repression. Because FBF binds the *fem-3 3' UTR* and is likely to be part of a cytoplasmic ribonucleoprotein complex that posttranscriptionally represses *fem-3*, one possibility is that *mep-1* could act on *fem-3* by regulating the expression of FBF. To test this hypothesis, we stained *mep-1* worms with anti-FBF antibodies. As shown in Figure 7, FBF-1 is normally expressed and localized in the cytoplasm around the nuclei of both wild-type and *mep-1* L4 larvae (Fig. 7A, C). Similar results were obtained for all the other developmental stages (not shown). As a consequence, our results indicate that *mep-1* is not required for correct processing, transport, and translation of the *fbf-1* RNA, as well as for the localization of the FBF-1 protein in the germline.

### DISCUSSION

In this study, we have identified the *C. elegans mep-1* gene and come to six major conclusions. First, the MEP-1 protein binds three MOG proteins, MOG-1, MOG-4, and MOG-5, as assayed both in yeast two-hybrid and in vitro experiments. Second, MEP-1 possesses seven putative zinc fingers and binds RNA nonspecifically. Third, similar to the MOG proteins, MEP-1 is a nuclear protein that is broadly expressed in both somatic and germline cells. Fourth, MEP-1 is re-

quired for multiple steps of development, including larval progression and gonadogenesis. Fifth, similar to the *mog* genes, MEP-1 is critical for *fem-3 3'-UTR*-mediated repression. Sixth, *mep-1* does not repress *fem-3* by promoting FBF-1 expression. The following discussion compares these MEP-1 characteristics with those of the MOG proteins, and suggests that MEP-1 and the MOG proteins act in a nuclear macromolecular complex to control mRNA activities.

### The functional relationship between MEP-1 and MOG proteins

What is the functional relationship between MEP-1 and the three MOG proteins in *C. elegans*? We consider several results that bear on this question. First, MEP-1 binds all three MOG proteins in yeast and in vitro. Second, all four are present in the same subcellular compartment, the nucleus (Puoti & Kimble, 1999; this work; unpubl. data). Third, both *mog* and *mep-1* genes are required maternally for viability of the next generation. Finally, and perhaps most importantly, all four are critical for repression of a reporter transgene that is controlled by the *fem-3 3' UTR* (Gallegos et al., 1998; this work). Together, these lines of evidence strongly support the idea that MEP-1 and the MOG proteins work together to control gene expression at the posttranscriptional level.

Although evidence described above suggests that the MEP-1 and MOG proteins work together, the *mep-1*

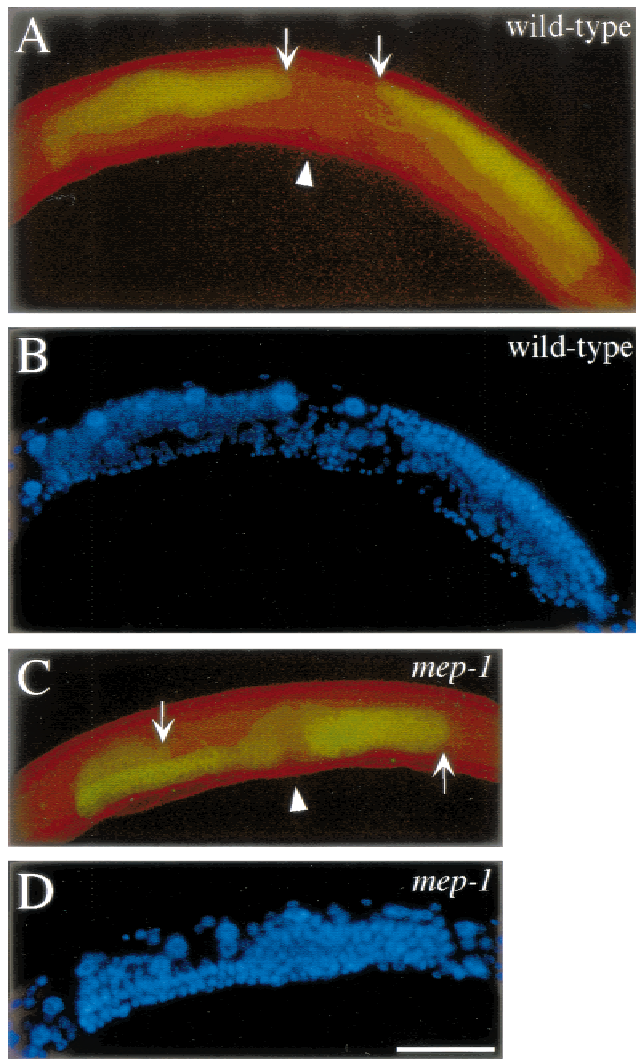


**FIGURE 7.** *mep-1* is not required for FBF-1 expression. Wild-type and *Mep-1* L4 larvae were stained with anti-FBF-1 antibodies. **A:** In wild-type worms, FBF-1 is detected in the cytoplasm that surrounds the dark nuclei of all immature germ cells. **B:** DNA staining of the same animal with DAPI; germ cell nuclei appear as tightly packed circles. **C:** anti-FBF-1 immunostaining of a L4 *Mep-1* hermaphrodite. As in wild-type animals, FBF-1 is present in the cytoplasm surrounding all germ cell nuclei, but is not found in the proximal gonad. **D:** DAPI staining of the same animal. Gonadal arms are not fully extended. Arrows point at the distal end of gonadal arms. The position of the developing vulva is indicated by an arrowhead. The bar represents 40  $\mu\text{m}$ .

and *mog* mutant phenotypes are not the same. The *mog* mutants have three primary defects: The germline is smaller than normal, the hermaphrodite germline fails to switch from spermatogenesis to oogenesis, and embryos produced by a homozygous *mog* mother are not viable (Graham & Kimble, 1993; Graham et al., 1993). The *mep-1* mutants, by contrast, have two primary defects: Gonadogenesis is aberrant in both somatic and germline tissues and embryos produced by a homozygous *mep-1* mother arrest during larval development. How do we think about the *Mep-1* and *Mog* mutant phenotypes, which superficially are so different?

The lines of evidence that MEP-1 and MOG proteins work together is strong (see above). One explanation for the different *mep-1* and *mog* phenotypes might have been that one or the other is not a null mutant. However, the *mep-1* deletion removes most of the coding region, including that encoding the zinc fingers and Q-rich domain, suggesting that this mutant is a null. Evidence that the *mog-1* phenotype is null is also strong (Puoti & Kimble, 1999). Therefore, this simple explanation cannot be invoked.

A second explanation for the different *mep-1* and *mog* mutant phenotype, which we favor, is that the *mep-1* gene has an overlapping role with the *mog* genes in development, but that each has distinct roles as well. The *mep-1* gonadogenesis defects demonstrate a critical role for this gene in development of the somatic gonad that is not observed for the *mog* genes. We conclude that *mep-1* plays a broader role in gonadogenesis than the *mog* genes. The germline defects of *mog* genes demonstrate a critical role for these genes in specification of germline fates. The same may be true for *mep-1*. Unfortunately, the severe gonadogenesis defects of *mep-1* mutants precluded a rigorous examination of its germline phenotype. Nonetheless, the *mep-1* expression in the germline together with its effect on PME-mediated gene regulation suggests that MEP-1 is required for development of both somatic and germline gonadal tissues.

### The MEP-1 and MOG proteins may form a macromolecular complex

The previous section suggested that MEP-1 and MOG proteins work together to control gene expression. In this section, we discuss the idea that these proteins may act in a macromolecular complex to execute their function. The physical interactions among these proteins support this idea. MEP-1 binds to each of the three MOG DEAH box proteins, and MEP-1 also interacts with itself. One simple model is that all four of these proteins are present together in a single complex. Alternatively, the MOG proteins might act sequentially, and MEP-1 might provide a physical and functional link among them. Experiments to distinguish between these models are in progress.

The MOG-1, MOG-4, and MOG-5 proteins are homologous to Prp2p, Prp16p, and Prp22p DEAH helicases in *S. cerevisiae*. These DEAH box helicases have been implicated in different steps of pre-mRNA splicing and transiently associate with the spliceosomal complex (Chen & Lin, 1990; Company et al., 1991; Schwer & Guthrie, 1991). MOG-1, MOG-4, and MOG-5 are the only homologs of Prp2p, Prp16p, and Prp22p in the nematode genome. Therefore, by analogy, one might expect that the MOG proteins are involved in splicing. However, attempts to investigate this possibility were negative (Puoti & Kimble, 1999). In contrast to what we

have observed for MOG-1 and MOG-5, protein–protein interactions have been reported between Prp16p and Prp22p (Nues & Beggs, 2001). Importantly, a recent study reported the physical interaction of the DEXH protein Brr2p with either Prp16p or Prp2p, the yeast MOG-1 and MOG-4 homologs, respectively (Nues & Beggs, 2001). To our knowledge, no interaction has been reported between Brr2p and Prp22p. Despite the fact that Brr2p has no structural homology to MEP-1 and that there is a close homolog of Brr2p in worms, MEP-1(FL) has similar binding properties to Brr2p, as it interacts with the Prp16p and Prp2p homologs MOG-1 and MOG-4. On the other hand, the Prp22p homolog MOG-5 does not bind to MEP-1(FL) in the yeast two-hybrid system, but does so *in vitro*. Therefore we cannot compare MEP-1(FL) and Brr2p in terms of their binding to MOG-5/Prp22p. We have shown that MEP-1(SH) binds to the three DEAH box MOG proteins *in vitro* and in the yeast two-hybrid system, but do not provide evidence that a shorter isoform of MEP-1 actually exists *in vivo*. No close MEP-1 homolog has been found in the yeast genome, but there is a MEP-1 homolog in *Drosophila*, suggesting that MEP-1 may have evolved among metazoans to link these three DEAH-box proteins.

### Possible roles of the MEP-1-MOG interaction

Although the *mog* genes are critical for PME-mediated regulation and for the hermaphrodite sperm/oocyte switch (Gallegos et al., 1998), little is known about how they might control *fem-3* mRNA activity. We now introduce MEP-1 as a part of the regulatory mechanism that controls *fem-3* expression. MEP-1 and the MOG proteins are likely to control many mRNAs, based on their complex mutant phenotypes, but *fem-3* is the only target so far identified. To date, we do not know how direct or indirect that control may be. The MEP-1 and MOG proteins are expressed in the nucleus and do not bind, at least specifically, to the PME (this study; A. Puoti, unpubl. results). MEP-1 binds RNA nonspecifically, and we have detected no preference for the PME. One possibility is that MEP-1 interacts with the *fem-3* 3' UTR nonspecifically and recruits other factors (e.g., the MOGs) to an RNP complex assembled on *fem-3* mRNA. Alternatively, MEP-1 and the MOGs may control other mRNAs or recruit other factors that have not yet been identified, and which in turn control *fem-3*. One possibility that is emerging is that two distinct complexes are required for *fem-3* repression, one nuclear complex that includes the MOG proteins and MEP-1, and another that is cytoplasmic and that contains FBF, NOS-3, and the *fem-3* mRNA. In this study, we present evidence that *mep-1* is not required for correct expression and localization of FBF, suggesting that either *mep-1* controls other target proteins that regulate *fem-3*, or that it is required for FBF activity rather than for FBF

expression. This would imply that MEP-1 and the MOG proteins can travel from the nucleus to the cytoplasm. An alternative possibility is that *mep-1* might act on *fem-3* in a way that is independent of the cytoplasmic complex. This hypothesis however, is not supported by genetical evidence that indicates that *fbf* and *mep-1* function in a nonredundant manner.

## MATERIALS AND METHODS

### Strains and expression constructs

*nT1[qIs50]* and *nT1[qIs51]* (referred to here as *nT1g*) and *DnT1[qIs50]* (*DnT1g*) were used as balancer chromosomes. *DnT1* (also called *nT1[unc(n574dm) let]*) is a dominant allele of *nT1*. *qIs50* is an insertion of *ccEx9747*, which drives expression of GFP in the pharynx, onto the *nT1* chromosome. *qIs19* is an insertion of *lag-2::GFP* (Blelloch et al., 1999). *qIs43* is an insertion of *LacZ::fem-3 3' UTR* (Gallegos et al., 1998).

The plasmids used for the yeast two- and three-hybrid experiments were pACT, pACTII, and pBTM116 (Bartel et al., 1993; Bai & Elledge, 1997). Yeast reporter strains were L40 (*MATa HIS3Δ200 trp-1-901 leu2-3,112 ade2 LYS2::(lexAop)4-HIS3 URA3::(lexAop)8-lacZ Gal4*) and L40-coat for the two- and three-hybrid assays, respectively (SenGupta et al., 1996; Vojtek et al., 1997). The *nos-3* cDNA in pACT was a gift from M. Wickens. The *nos-3* cDNA is truncated on its 5' end in that it is missing the region corresponding to the first 41 amino acids. All constructs were sequenced at least on the 5' cloning site to verify the reading frame.

For *in vitro* translation, we used the pCITE vector (Novagen). Full length *mog-1*, *-4*, and *-5*, and *mep-1* cDNAs were cloned with their 5' end in frame. To obtain fusion proteins with GST, *mep-1* (SH and FL), *fbf-1*, and *mog-4* were cloned into pGEX5-3a (Amersham-Pharmacia) and expressed in BL21 bacteria. Recombinant protein was purified according to the manufacturer's recommendations (Amersham-Pharmacia).

### Characterization of the *mep-1* full-length cDNA

The program Genefinder (L. Hillier & P. Green, unpubl.) predicted the full-length MEP-1 protein to be made of 853 amino acids. We isolated several cDNAs of *mep-1* and found that the full-length *mep-1* cDNA actually encodes a protein of 870 amino acids. This discrepancy is due to a predicted 51-nt intron that is present in fully spliced cDNAs. The supplemental 51 nt do not perturb the reading frame, nor generate a premature stop codon. The 5' end of the *mep-1* cDNA was obtained by PCR. For the 5' end, semi-nested PCR was performed on single-stranded cDNA using SL1 or SL2 sense primers and two antisense primers (GAATGCTGGGATCCA ATTGG and GAACTTTGTCCAGGATCAGC) that are specific to *mep-1*. SL1 and SL2 are *trans*-spliced leaders that are present on the 5' end of many *C. elegans* cDNAs. Only SL1 gave a product, which was sequenced and identified as the 5' end of *mep-1*.

### Yeast two- and three-hybrid methods

The random-primed  $\lambda$ ACT-RB2 cDNA library from mixed staged *C. elegans* hermaphrodites was converted to plasmid by Cre-dependent recombination in the RB4E *Escherichia coli* strain. Yeast cells were transformed and selected on synthetic complete media (SD) lacking the appropriate amino acid (Trp for pBTM116-derived constructs, Leu for pACT-derived constructs). The library transformations were plated on SD Trp<sup>-</sup> Leu<sup>-</sup> His<sup>-</sup> with 5 mM of 3-amino-1,2,4-triazole. For each screen, 100  $\mu$ g of plasmid library was used to transform L40 yeast strains carrying the bait vector. Colonies were picked after 3 to 6 days and retested for their ability to grow in the absence of His and for their  $\beta$ -Gal activity. From the screens with MOG-1 and MOG-5, 17 and 24 clones, respectively, that were positive for HIS and LACZ expression were obtained. To detect  $\beta$ -Gal activity, yeast colonies were lifted and processed as described (Bai & Elledge, 1997). X-gal was used at a concentration of 1 mg/mL. Filters were incubated at 30 °C and monitored frequently for the appearance of blue staining. All transformations and colony lift assays were performed at least five times on isolated colonies. To verify that the proteins were produced in yeast, their presence was verified by western blotting using anti-MEP-1 antibodies and antibodies directed against the LexA DNA binding domain and the Gal4 activation domain (Upstate Biotechnology).

### In vitro binding assays

[<sup>35</sup>S Met]-labeled full-length MOG and MEP-1 proteins were produced by in vitro translation (Promega). Cold MOG-4, FBF-1, and MEP-1 (SH or FL) GST fusion proteins were extracted from *E. coli* strain BL21 and bound to glutathione-Sepharose beads. For pull-down assays, 5  $\mu$ L of beads were added to 3  $\mu$ L of the in vitro-synthesized protein and incubated for 3 h at 4 °C in 300  $\mu$ L of binding buffer under gentle rocking. Beads were washed several times with binding buffer and bound proteins were analyzed by SDS-PAGE. The gel was dried and autoradiographed. RNase treatments were performed at 30 °C for 30 min by adding 75  $\mu$ g of RNase A to 3  $\mu$ L of in vitro translation mixture. Controls were mock incubated with water instead of RNase. Interaction assays between MOG-1 and MEP-1, between MOG-5 and MEP-1, and the corresponding controls with GST alone and FBF-1-GST were done in 20 mM HEPES, pH 7.5, 50 mM NaCl, 2 mM DTT, 2 mM MgCl<sub>2</sub>, 0.5% nonfat dry milk. For MOG-MOG, MOG-4-MEP-1, and MEP-1-MEP-1 interactions and the corresponding controls, the binding buffer was 20 mM HEPES, pH 7.5, 75 mM KCl, 1 mM EDTA, 2 mM DTT, 2 mM MgCl<sub>2</sub>, and 0.5% NP40.

### Northern analysis

Poly(A)<sup>+</sup> RNA was extracted as previously described (Puoti & Kimble, 1999). For northern analysis, 3  $\mu$ g of poly(A)<sup>+</sup> RNA was run on a 1.2% denaturing agarose glyoxal gel in 10 mM sodium phosphate at pH 7.0 and transferred to N-Hybrid Nylon membrane (Amersham) in 10 $\times$  SSC. Pre-hybridization and hybridization were done as described (Puoti & Kimble, 1999). Blots were probed with a 922-nt *Pvu*II *mep-1* cDNA fragment.

### Generation of a *mep-1* deletion mutant

L4 hermaphrodites were treated with 30 mg/mL of trimethylpsoralen in M9 buffer for 15 min at room temperature and irradiated for 90 s at 340 mW/cm of UV light (360 nm) under gentle shaking. Treated animals were cultured at 20 °C for 1 day at room temperature for self-fertilization, and then treated with basic hypochlorite to collect the eggs (F1 generation). The F1 were allowed to hatch and were divided into 1,152 groups of 500 animals. After 5 days of culture, each group served for the preparation of genomic DNA. The DNA was used as a template for nested PCR using two pairs of oligonucleotides. Pair one (outer pair, AP189s and AP190a, 5'-CCACGTTTGATACTCAGTCAC and 5'-GTATACTGATCTGTCTTATGGG) served to amplify a region of 3,396 nt that spans the whole *mep-1* open reading frame. The second pair was used for nested PCR and amplified a 3,202-nt fragment (inner pair, AP191s and AP192a, 5'-GCCTATTTCTCACTA TCTAGA and 5'-ACATGATAATTGTGGGGTAGTTA). A population that contained a mutant that generated a PCR signal of 1 kb instead of 3.2 kb was repeatedly subdivided into smaller pools, until heterozygotes carrying the deletion were isolated. The mutant allele, *mep-1(q660)* was outcrossed several times before phenotypic analysis.

### RNA interference

A 922-nt *Pvu*II *mep-1* cDNA fragment was cloned into pBlue-script, linearized, and used as a template for in vitro transcription with T3 and T7 RNA polymerase (Stratagene). To obtain double-stranded cRNA, equimolar amounts of sense and antisense RNA were annealed for 10 min at 68 °C in 6.6 mM potassium phosphate, pH 7.3, 1 mM potassium citrate, pH 7.5, and 0.66% PEG 6000, followed by 30 min at 37 °C. Young wild-type adult worms were microinjected with 1 to 2  $\mu$ g/ $\mu$ L of dsRNA and transferred every 12 to 24 h to a fresh plate.

### Phenotypic characterization of the *mep-1* deletion allele

The entire broods of strains AP5 (*mep-1(q660)unc-22(e66)/dpy-20(e1362)*) and JK2906 (*(mep-1(q660)/nT1([qls51]; (aka nT1g))*) were analyzed at 15 °C, 20 °C, and 25 °C. Young hermaphrodites were singled and their progenies were scored. If an egg did not hatch after 2 days, it was considered as dead. Larvae that did not progress in their development for 3 days were considered as arrested.

To visualize germline and somatic nuclei, worms were stained with diamidino-phenylindole (DAPI; 0.5  $\mu$ g/mL in ethanol). Nuclei from immature germ cells and sperm were counted under fluorescence. To obtain the total number of germ cells, the number of sperm nuclei was divided by four and added to the counts of immature germ cell nuclei. *n* represents the number of animals scored.

We scored distal tip cells (DTC) using a combination of *lag-2::GFP* expression (Blelloch et al., 1999), cellular morphology, and gonadal arm elongation. *mep-1(q660)* mutants often have weak *lag-2::GFP* expression and reduced arm elongation, so we relied upon all of above the criteria to more accurately count the number of DTCs. To count the number

of somatic cells at the somatic gonadal primordium stage, we synchronized *mep-1(q660)unc-22(e66)/DnT1[qIs51]; qIs19/DnT1[qIs51]* and allowed them to develop until early L3. Non-green worms are *mep-1(q660)* and express *lag-2::GFP*, which was used to count somatic cells. At this stage, *lag-2::GFP* is dimly expressed in all of the somatic cells of the gonad, but not the germ cells. No gonadal defects were observed in *unc-22(e66)* mutants (not shown).

## Antibodies

Polyclonal antibodies were raised against the C-terminal portion of MEP-1 by injecting a rabbit with a synthetic Keyhole limpet hemocyanin-coupled peptide. The sequence of the peptide was TSNHPKGDKKTSTPAKKDDC. For immunostaining, worms at different developmental stages were fixed as described (Bettinger et al., 1996) and stained in PTB (1% BSA, 1 mM EDTA, 0.5 Triton-X-100, and 0.05% NaN<sub>3</sub> in PBS) using a 1/200 dilution of serum. The secondary antibody (anti-rabbit FITC-conjugated; Jackson ImmunoResearch Laboratories) was added at a dilution of 1/1,000 in PTB. After 16 h at 4 °C, worms were washed and mounted on slides with vectashield and DAPI. No nuclear staining was detected with preimmune serum. DAPI staining of nuclei that were already stained by anti-MEP-1 antibodies was consistently weak, possibly because staining with anti-MEP-1 antiserum interferes with DAPI staining (Fig. 4G). Anti-FBF-1 antibodies have previously been described (Zhang et al., 1997). Western blot analysis was done with 5 to 10 mg of total protein extracts from wild-type, *fem-3(e1996)* loss-of-function adults, and *mep-1(q660)* mutant worms run on a denaturing 7.5% polyacrylamide gel. Blots were incubated in Blotto/Tween with affinity-purified anti-MEP-1 antibodies at a final dilution of 1 to 150. These anti-MEP-1 antibodies were directed against the full-length MEP-1 protein and affinity purified on recombinant full-length MEP-1. The secondary antibody (anti-rabbit HRP-conjugated; Sigma) was used at a dilution of 1 to 15,000.

## Generation of transgenic animals and scoring of reporter expression

### *mep-1::GFP fusion*

A 5,874-nt *SwaI/SmaI* fragment from cosmid M04B2 was cloned into pBluescript. This genomic clone contained the whole coding sequence for *mep-1*, including 2,358 nt of 5' flanking and 648 nt of 3' flanking genomic sequence. A *HpaI* site was created by PCR near the *mep-1* stop codon to introduce a 1,010-nt genomic fragment coding for GFP (nucleotides GATTAA were mutated into GTTAAC; the *mep-1* stop codon is shown in bold). The stop codon of the fusion construct was that of GFP. The 5' and 3' flanking and untranslated regions of the GFP construct were those of *mep-1* (Fig. 1A). The 5' flanking sequence should contain all the elements of the *mep-1* promoter, as the *mep-1::GFP* construct can rescue *mep-1(q660)* in that fertile Unc progeny were obtained from injected *mep-1(q660)unc-22(e66)/dpy-20(e1362)* hermaphrodites. *mep-1* heterozygotes were injected with *mep-1::GFP* at a concentration of 8 ng/μL and GFP expression was monitored by epifluorescence in iso-

lated lines. The array was integrated by irradiation with 30,000 μJ at 254 nm.

### *lacZ::fem-3 3' UTR*

The *lacZ::fem-3 3' UTR* transgene has been described earlier (Gallegos et al., 1998). The *lacZ::fem-3 3' UTR* construct was injected along with pRF4 and integrated by gamma radiation to generate *qls43. qls43/+* males were crossed into *mep-1(q660)/DnT1* heterozygotes and rolling progeny of genotype *mep-1(q660)/+ ; qls43* was isolated. Plates segregating 25% of Mep-1 rolling animals were used for expression studies: 20 to 30 Mep-1 (*mep-1/mep-1*) and wild-type (*mep-1/+* or *+/+*) adults were picked together on a single plate and heat-shocked for 2 h at 33 °C, followed by a 2-h recovery at 25 °C. Mep-1 homozygotes were selected upon the absence of embryos and a protruding vulva. Staining for β-Gal was done for 12–16 h at 37 °C. Stained animals were scored by counting the number of somatic nuclei with strong blue color. The head region was not scored because it had background staining and because small nuclei in the head were difficult to count. Therefore, we only counted stained nuclei in the region that spans the posterior end of the pharynx to the posterior end of the animal. Embryos in wild-type animals with occasional strong blue color were not included in the counts. Experiments with the *LacZ::tra-2(+)* reporter strain were done as described above, except that all blue nuclei were counted (Goodwin & Evans, 1997). The results from all experiments are presented independently, as variations were observed between the heat-shock and staining procedures.

## ACKNOWLEDGMENTS

We gratefully acknowledge Craig Mello and Yingdee Unhavaithaya for communicating results prior to publication and for sharing affinity-purified MEP-1 antibody. Thanks go to Andy Fire for constructs, Frédéric Guerry for advice on Pn.p induction, and Zary Saudan and Verena Zimmermann for technical assistance. We are grateful to Betsy Goodwin for sharing the *tra-2* reporter strain. A.P. was supported by the Sandoz Foundation (Grant 98C44) and the Swiss National Science Foundation (Grants 3100-055384.98/1 and 3130-054989.98/1). J.K. is an investigator of the Howard Hughes Medical Institute.

Received November 21, 2001; returned for revision  
January 3, 2002; revised manuscript received  
March 19, 2002

## REFERENCES

- Ahringer J, Kimble J. 1991. Control of the sperm-oocyte switch in *Caenorhabditis elegans* hermaphrodites by the *fem-3 3'* untranslated region. *Nature* 349:346–348.
- Austin J, Kimble J. 1987. *glp-1* is required in the germ line for regulation of the decision between mitosis and meiosis in *C. elegans*. *Cell* 51:589–599.
- Bai C, Elledge SJ. 1997. Searching for interacting proteins with the two-hybrid system I. In: Bartel PL, Fields S, eds. *The yeast two-hybrid system*. Oxford: Oxford University Press. pp 11–28.
- Bartel P, Chien C, Sternglanz R, Fields S. 1993. Using the two-hybrid system to detect protein–protein interactions. In: Hartley DA, ed. *Cellular interactions in development: A practical approach*. Oxford: Oxford University Press. pp 153–179.

- Barton MK, Schedl TB, Kimble J. 1987. Gain-of-function mutations of *fem-3*, a sex-determination gene in *Caenorhabditis elegans*. *Genetics* 115:107–119.
- Bettinger JC, Lee K, Rougvie AE. 1996. Stage-specific accumulation of the terminal differentiation factor LIN-29 during *Caenorhabditis elegans* development. *Development* 122:2517–2527.
- Bielloch R, Anna-Arriola SS, Gao D, Li Y, Hodgkin J, Kimble J. 1999. The *gon-1* gene is required for gonadal morphogenesis in *Caenorhabditis elegans*. *Dev Biol* 216:382–393.
- Chen JH, Lin RJ. 1990. The yeast PRP2 protein, a putative RNA-dependent ATP-ase, shares extensive sequence homology with two other pre-mRNA splicing factors. *Nucleic Acids Res* 18:6447.
- Company M, Arenas J, Abelson J. 1991. Requirement of the RNA helicase-like protein PRP22 for release of messenger RNA from spliceosomes. *Nature* 349:487–493.
- Evans TC, Crittenden SL, Kodoyianni V, Kimble J. 1994. Translational control of maternal *glp-1* mRNA establishes an asymmetry in the *C. elegans* embryo. *Cell* 77:183–194.
- Fire A, Albertson D, Harrison SW, Moerman DG. 1991. Production of antisense RNA leads to effective and specific inhibition of gene expression in *C. elegans* muscle. *Development* 113:503–514.
- Fire A, Xu S, Montgomery MK, Kostas SA, Driver SE, Mello CC. 1998. Potent and specific genetic interference by double-stranded RNA in *Caenorhabditis elegans*. *Nature* 391:806–811.
- Gallegos M, Ahringer J, Crittenden S, Kimble J. 1998. Repression by the 3' UTR of *fem-3*, a sex-determining gene, relies on a ubiquitous *mog*-dependent control in *Caenorhabditis elegans*. *EMBO J* 17:6337–6347.
- Goodwin EB, Evans TC. 1997. Translational control of development in *C. elegans*. *Semin Cell Dev Biol* 8:551–559.
- Goodwin EB, Okkema PG, Evans TC, Kimble J. 1993. Translational regulation of *tra-2* by its 3' untranslated region controls sexual identity in *C. elegans*. *Cell* 75:329–339.
- Graham PL, Kimble J. 1993. The *mog-1* gene is required for the switch from spermatogenesis to oogenesis in *Caenorhabditis elegans*. *Genetics* 133:919–931.
- Graham PL, Schedl T, Kimble J. 1993. More *mog* genes that influence the switch from spermatogenesis to oogenesis in the hermaphrodite germ line of *Caenorhabditis elegans*. *Dev Genet* 14:471–484.
- Hodgkin J. 1986. Sex determination in the nematode *Caenorhabditis elegans*: Analysis of *tra-3* suppressors and characterization of the *fem* genes. *Genetics* 114:15–52.
- Kimble J, Hirsh D. 1979. The postembryonic cell lineages of the hermaphrodite and male gonads in *Caenorhabditis elegans*. *Dev Biol* 70:396–417.
- Kimble J, Ward S. 1988. Germ line development and fertilization. In: Wood WB, ed. *The nematode Caenorhabditis elegans*. Cold Spring Harbor, New York: Cold Spring Harbor Laboratory Press. pp 191–213.
- Kimble JE, White JG. 1981. On the control of germ cell development in *Caenorhabditis elegans*. *Dev Biol* 70:396–417.
- Kraemer B, Crittenden S, Gallegos M, Moulder G, Barstead R, Kimble J, Wickens M. 1999. NANOS-3 and FBF proteins physically interact to control the sperm-oocyte switch in *Caenorhabditis elegans*. *Curr Biol* 9:1009–1018.
- Lee RC, Feinbaum RL, Ambros V. 1993. The *C. elegans* heterochronic gene *lin-4* encodes small RNAs with antisense complementarity to *lin-14*. *Cell* 75:843–854.
- McCarter J, Bartlett B, Dang T, Schedl T. 1997. Soma-germ cell interactions in *Caenorhabditis elegans*: Multiple events of hermaphrodite germline development require the somatic sheath and spermathecal lineages. *Dev Biol* 181:121–143.
- Mickey KM, Mello CC, Montgomery MK, Fire A, Priess JR. 1996. An inductive interaction in 4-cell stage *C. elegans* embryos involves APX-1 expression in the signalling cell. *Development* 122:1791–1798.
- Moss EG, Lee RC, Ambros V. 1997. The cold shock domain protein LIN-28 controls developmental timing in *C. elegans* and is regulated by the *lin-4* RNA. *Cell* 88:637–646.
- Nues RW, Beggs JD. 2001. Functional contacts with a range of splicing proteins suggest a central role for Br2p in the dynamic control of the order of events in spliceosomes of *Saccharomyces cerevisiae*. *Genetics* 157:1451–1467.
- Puoti A, Kimble J. 1999. The *Caenorhabditis elegans* sex determination gene *mog-1* encodes a member of the DEAH-box protein family. *Mol Cell Biol* 19:2189–2197.
- Puoti A, Kimble J. 2000. The hermaphrodite sperm/oocyte switch requires the *Caenorhabditis elegans* homologs of PRP2 and PRP22. *Proc Natl Acad Sci USA* 97:3276–3281.
- Schwer B, Guthrie C. 1991. PRP16 is an RNA-dependent ATPase that interacts transiently with the spliceosome. *Nature* 349:494–499.
- SenGupta DJ, Zhang B, Kraemer B, Pochart P, Fields S, Wickens M. 1996. A three-hybrid system to detect RNA–protein interactions in vivo. *Proc Natl Acad Sci USA* 93:8496–8501.
- Slack FJ, Basson M, Liu Z, Ambros V, Horvitz HR, Ruvkun G. 2000. The *lin-41* RBCC gene acts in the *C. elegans* heterochronic pathway between the *let-7* regulatory RNA and the LIN-29 transcription factor. *Mol Cell* 5:659–669.
- Vojtek AB, Cooper JA, Hollenberg SM. 1997. Searching for interacting proteins with the two-hybrid system. In: Bartel PL, Fields S, eds. *The yeast two-hybrid system*. Oxford: Oxford University Press. pp 29–42.
- Wickens M, Goodwin EB, Kimble J, Strickland S, Hentze MW. 2000. Translational control of developmental decisions. In: Sonenberg JW, Hershey B, Mathews MB, eds. *Translational control of gene expression*. Cold Spring Harbor, New York: Cold Spring Harbor Laboratory Press. pp 295–370.
- Zhang B, Gallegos M, Puoti A, Durkin E, Fields S, Kimble J, Wickens MP. 1997. A conserved RNA-binding protein that regulates sexual fates in the *C. elegans* hermaphrodite germ line. *Nature* 390:477–484.